

Antiferromagnetic phase in β' -(BEDT-TTF) $_2$ ICl $_2$ under pressure as seen via ^{13}C NMR

Yoshihiro Eto and Atsushi Kawamoto*

Department of Quantum and Condensed Matter Physics, Graduate School of Science, Hokkaido University, Kita-ku, Sapporo, Hokkaido 060-0810, Japan

(Received 27 September 2009; revised manuscript received 15 December 2009; published 28 January 2010)

We assessed carbon-13 nuclear magnetic resonance (^{13}C NMR) measurements of the layered organic salt β' -(BEDT-TTF) $_2$ ICl $_2$, which exhibits antiferromagnetic transition at ambient pressure and 22 K and superconductive transition at 8.2 GPa and 14.2 K (the highest known superconductive transition temperature among organic superconductors). By analyzing the ^{13}C NMR spectrum with the tensor, we determined the antiferromagnetic moment of this salt to be μ_B per dimer at ambient pressure, strongly indicating that this salt is a dimer Mott insulator. From NMR measurements under pressure, we found that the structure of the antiferromagnetic phase changed at 0.6 GPa. The moment of this antiferromagnetic phase was estimated to be $0.47\mu_B$ per dimer at 0.6 GPa and 26 K. In addition, applying pressure rapidly decreased the spin susceptibility in the paramagnetic state, and the pressure dependence of T_N showed anomalous behavior consistent with theoretical proposals, including dimensional crossover.

DOI: [10.1103/PhysRevB.81.020512](https://doi.org/10.1103/PhysRevB.81.020512)

PACS number(s): 74.70.Kn, 76.60.-k, 82.80.Gk

For unconventional superconductors, including high- T_c superconductors, two conflicting descriptions can be used to illustrate the electronic structure. One originates from a Mott insulator, explaining the strong limit of the onsite Coulomb interaction U , whereas the other incorporates the electronic correlation into the itinerant electron system, which has a large transfer energy t . Among the organic superconductors, (BEDT-TTF) $_2X$ superconductors, where BEDT-TTF is bis(ethylenedithio)-tetrathiafulvalene and X is a monovalent counter anion, have been thoroughly investigated. The combination of BEDT-TTF and inorganic ions forms two-dimensional conducting sheets with various crystal structures. Of these, the salts typified by κ -(BEDT-TTF) $_2X$ have been used to assess the relationship between antiferromagnetism and superconductivity provided by the two conflicting descriptions mentioned above.¹⁻³

Recently, the superconductivity of β' -(BEDT-TTF) $_2$ ICl $_2$ under pressure was examined.⁴ In crystals of this salt, the BEDT-TTF molecules form a conduction layer and the ICl $_2$ anions form an insulating layer; these layers alternate with each other [Fig. 1(a)]. Magnetically, this salt shows anisotropic susceptibility at 22 K and ambient pressure (ap), indicating that the antiferromagnetic transition occurs at this temperature.⁵ Moreover, this antiferromagnetic phase is thought to arise from simple up-down sites revealed by neutron magnetic scattering.⁶ Due to the commensurate antiferromagnetic transition of this salt and the strong dimer structure with one carrier, the Mott insulator picture may fit this salt better. Electrically, this salt shows semiconductive behavior below room temperature at ambient pressure. Its resistivity can be suppressed by applying pressure, causing the insulating phase to disappear and the superconductive transition to occur at 14.2 K under 8.2 GPa.⁴ This is the highest known transition temperature among organic superconductors. Metallization and superconductivity under pressure, which are the properties of a Mott insulator, were expected.

Alternatively, however, the mechanism of superconductivity is thought to involve antiferromagnetic fluctuations induced by changing the dimensionality of the Fermi

surface.^{1,7} Many β -(BEDT-TTF) $_2X$ salts show superconductivity, and these salts have also been thoroughly investigated.⁸⁻¹⁵ In both the β and β' type salts, the BEDT-TTF molecules form dimers that are parallel to each other. In the β type, the dimers form a linear arrangement; however in the β' type, the dimers are slightly skewed. Therefore, it is generally believed that β' -type salts are more strongly dimerized than β -type salts.¹⁶⁻¹⁸ An alternative description is based on the structural deformation from β' structure to β structure. Indeed, this structural deformation is suggested by a first-principle theoretical calculation.¹⁹ This description suggests that the application of pressure initially increases but then decreases the antiferromagnetic transition temperature T_N , resulting in superconductivity. In a simple Mott insulator, T_N is likely to decrease when pressure is applied. For this salt, however, nothing is known about the actual behavior of T_N under pressure.

Nuclear magnetic resonance (NMR) has several advantages, including the ability of the spectrum to detect the internal field during antiferromagnetic transition, and the abil-

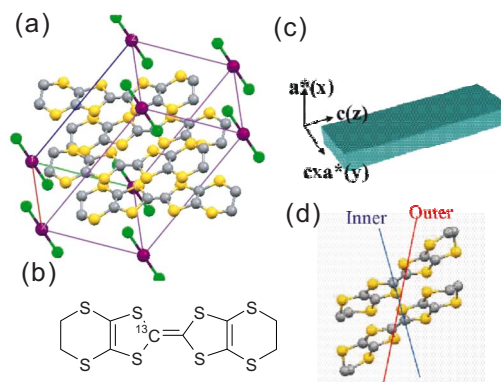


FIG. 1. (Color online) (a) Crystal structure of β' -(BEDT-TTF) $_2$ ICl $_2$. (b) BEDT-TTF molecule enriched with ^{13}C isotopes on only one side of the central carbon sites. (c) Crystal shape as well as x , y , and z axes defined by us. (d) Dimeric structure with site definition of the central C=C carbons.

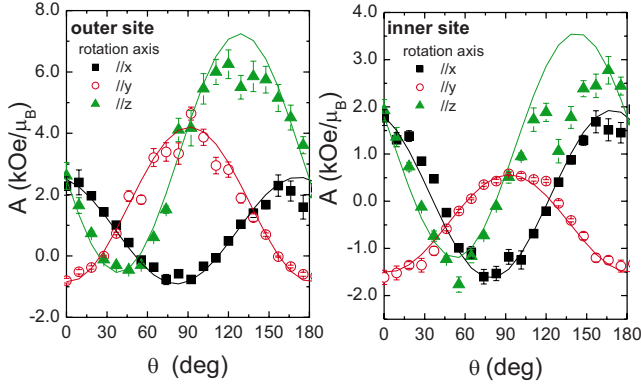


FIG. 2. (Color online) Angular dependence of the hyperfine coupling constant. Solid lines represent calculated value.

ity to measure spin susceptibility under pressure as a Knight shift using the hyperfine coupling constant. We therefore measured ^{13}C NMR with a special enriched molecule with ^{13}C nuclei to determine the hyperfine coupling tensors. Additionally, we investigated the electronic state of this salt microscopically, the pressure dependence of T_N , and the amplitude of the moment, in order to determine the accuracy of the two conflicting descriptions of electronic structure in unconventional superconductors.

For our analysis, we utilized a single crystal of β' -(BEDT-TTF) $_2\text{ICl}_2$, in which one side of the central carbon nuclei in the BEDT-TTF molecules were replaced by ^{13}C nuclei [Fig. 1(b)].²⁰ NMR measurements were performed with decreasing temperature under a field of 9.4 T and under pressures ranging from ambient pressure to 3.0 GPa using a clamp cell made of NiCrAl alloy. Daphni oil 7373 was used as the pressure medium. NMR spectra were obtained by fast Fourier transformation (FFT) of the echo signal with a pulse width of $\pi/2$ of 4 μs . NMR spectra obtained during the antiferromagnetic phase were merged with FFT spectra at 50 kHz intervals. Spin-lattice relaxation time was determined by the saturation recovery method.

We measured the temperature dependence of the NMR shift from 40 to 100 K with the three axes of rotation at ambient pressure and evaluated the hyperfine coupling constant in each direction using χ - δ plots. We defined the x , y , and z axes from the shape of the single crystal in Fig. 1(c). There are two crystallographic nonequivalent inner and outer sites [Fig. 1(d)] because BEDT-TTF forms a dimer in the sheet. Indeed, two NMR spectral peaks were observed in all three axes of rotation. Figure 2 shows the angular dependence of the hyperfine coupling constant obtained from the slope of the χ - δ plot. Thus, we determined the hyperfine coupling tensors:

$$\mathbf{A}_{\text{inner}} = \begin{pmatrix} 0.56 & 2.3 & 0.08 \\ 2.3 & 1.8 & 0.70 \\ 0.08 & 0.70 & -1.5 \end{pmatrix} \mathbf{A}_{\text{outer}} = \begin{pmatrix} 4.2 & 3.8 & 0.12 \\ 3.8 & 2.5 & 0.60 \\ 0.12 & 0.60 & -0.84 \end{pmatrix}$$

kOe/ μ_B per BEDT-TTF dimer unit.

After obtaining these hyperfine coupling tensors, we could calculate the structure of the antiferromagnetic phase at ambient pressure. As previously reported, a divergence of

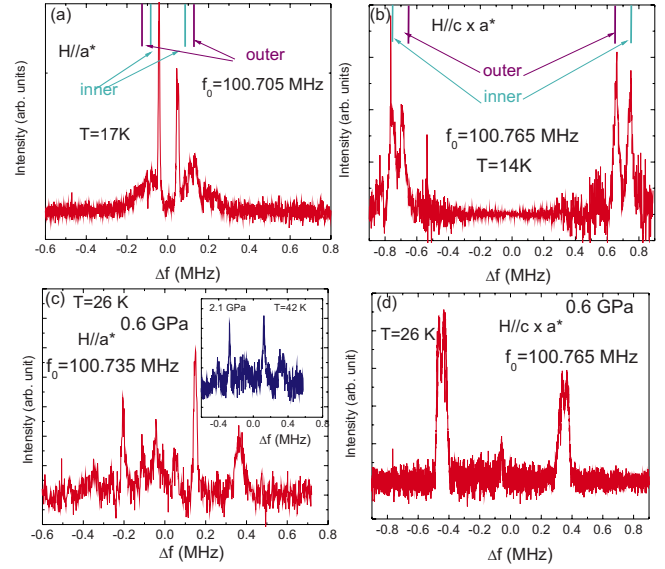


FIG. 3. (Color online) NMR spectra below the antiferromagnetic transition temperature at (a) $H\parallel a^*$ and (b) $H\parallel c \times a^*$. Solid lines are the calculated positions with moments of 1 μ_B per dimer. (c) NMR spectrum below the antiferromagnetic transition temperature at 0.6 GPa and $H\parallel a^*$. The inset shows the NMR spectrum at 2.1 GPa. (d) NMR spectrum below the antiferromagnetic transition temperature at 0.6 GPa and $H\parallel c \times a^*$.

$(T_1T)^{-1}$ was observed at 22 K.²¹ In order to investigate the amplitude of the antiferromagnetic moment, we applied external fields parallel to the a^* and $c \times a^*$ axes. Spin flopping did not occur in these configurations. Therefore, the antiferromagnetic moment forms an internal field parallel to the a^* and $c \times a^*$ axes via the off-diagonal elements A_{13} and A_{23} of the hyperfine coupling tensor. Figures 3(a) and 3(b) show the observed spectra in both configurations. Four symmetrical peaks were observed, indicating a commensurate structure in which the inner and outer sites were each split into two sites by differences in internal fields caused by the simple up and down moments. These findings were consistent with the results of neutron magnetic scattering.⁶ The amplitude of the moment provides important information. Assuming that the amplitude of the moment is μ_B per dimer, the peaks could be assigned in both directions by using either of the hyperfine coupling constants A_{13} or A_{23} (Fig. 3). When the Mott insulator picture is suitable, the moment should almost be μ_B per dimer. The Mott insulator model can also explain that the Curie constant of the high-temperature paramagnetic phase and the spin per dimer is $S = \frac{1}{2}$.

Our main purpose was to determine how the antiferromagnetic phase changed when pressure was applied. From the Mott insulator picture at ambient pressure, we expected that T_N would decrease with increased pressure. We therefore measured NMR spectra and T_1 up to 3.0 GPa with an external field parallel to the a^* axis.

We observed a different antiferromagnetic structure above 0.3 GPa. Figures 3(c) and 3(d) show the NMR spectrum below the antiferromagnetic transition at 0.6 GPa. This spectrum consisted of seven or eight peaks. However, as shown in the inset of Fig. 3(c), applying more pressure suppressed

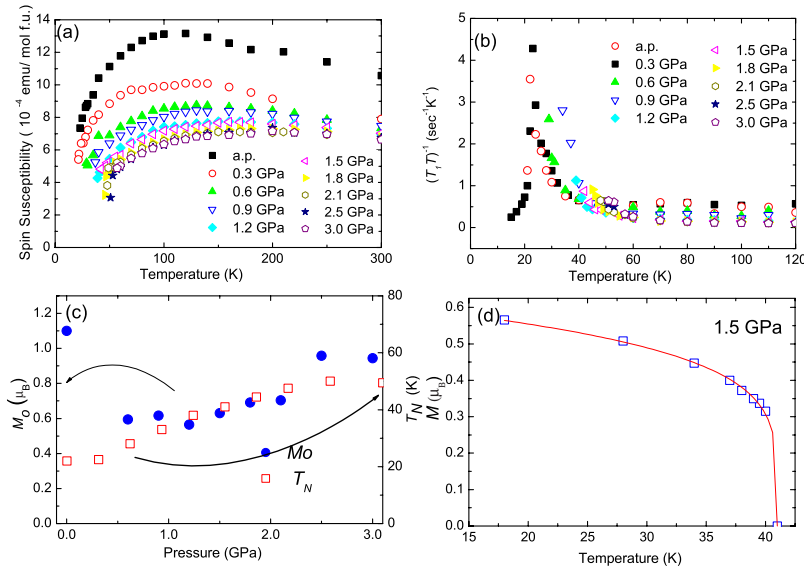


FIG. 4. (Color online) (a) Temperature dependence of the spin susceptibility at ap and higher pressures. (b) Temperature dependence of $(T_1T)^{-1}$ at ambient pressure and higher pressures. (c) Pressure dependence of the staggered moment and T_N . (d) Temperature dependence of the staggered moment at 1.5 GPa.

the structure around 0 MHz. Thus, four primary peaks were observed in the high-pressure region. This result suggested that two different magnetic phases coexisted at 0.6 GPa and that the phase with the smaller internal field disappeared when more pressure was applied. Similar to ambient pressure, the remaining phase under high pressure consisted of four peaks. Whereas the splitting width at $H\parallel a^*$ was about twice that at ambient pressure, the splitting width at $H\parallel c \times a^*$ was about half that at ambient pressure, as shown in Fig. 3(d). These results cannot be explained only by changes in the magnitude of the moment but by changes in the magnetic structure. The moment should be perpendicular to an external field under 9.4 T because the flop field of this salt is less than 1 T at ambient pressure.⁵ We estimated that at 0.6 GPa, the amplitude of the moment was $0.47\mu_B$ per dimer, and the direction of the moment was 22.7° from the c axis for $H\parallel a^*$ and 8.07° from the c axis for $H\parallel c \times a^*$.

We should be able to observe the changes corresponding to these alternations in the high-temperature paramagnetic phase. NMR can detect spin susceptibility as the Knight shift: spin susceptibility can be calculated by dividing the Knight shift by the hyperfine coupling constant. Figure 4(a) shows the spin susceptibility of the paramagnetic phase obtained from the Knight shift under pressure. The spin susceptibility decreased significantly, about 30%, from ambient pressure to 0.6 GPa, and the hump structure present around 100 K was suppressed. Under higher pressures, the spin susceptibility decreased slightly. These findings indicated that the paramagnetic phase under pressure was significantly altered from that at ambient pressure. While acting as a semiconductor at 2.0 GPa, its conductivity at room temperature increased by two orders of magnitude,⁴ indicating that its itinerancy had increased.

In this antiferromagnetic phase, T_N under pressure was determined as the temperature at which the spectrum was changed by a difference in the internal field. At 0.3, 0.6, 0.9, 1.2, 1.5, 1.8, 2.1, 2.5, and 3.0 GPa, the spectrum changed at 22.5, 28, 33, 38, 41, 44.5, 47.5, 50.0, and 49.5 K, respectively; divergences of $(T_1T)^{-1}$ were also observed at these respective temperatures, as shown in Fig. 4(b). As illustrated

in Fig. 4(c), the transition temperature almost doubled as pressure increased up to 2.5 GPa, and then it became saturated or slightly decreased as further pressure was applied. In the Mott insulator, applying pressure corresponds to controlling W/U , where W is the bandwidth. Thus, the system is predicted to come close to the metallic state, with T_N decreasing at higher pressure. Actually, however, T_N increased at higher pressure: T_N at 2.5 GPa was more than double T_N at 0.3 GPa.

We also evaluated the staggered moment in the antiferromagnetic phase by fitting the temperature dependence of the moment at each pressure using the formula $M(T) = M_0(1 - T/T_N)^\beta$ [Fig. 4(d)]. As shown in Fig. 4(b), the staggered moment increased as T_N increased.

At ambient pressure, the Mott model is thought to be suitable. T_N , however, increased at higher pressure. This anomalous increase in T_N corresponds to the prediction made by the band model.^{1,7,19} Due to the magnetic phase under pressure and the rapid decrease in spin susceptibility at higher pressure, the Mott model at ambient pressure was not directly connected to the electronic structure under pressure, indicating that the band model may be more suitable at higher pressure. In κ -(BEDT-TTF)₂Cu[N(CN)₂]X, there is no significant change in spin susceptibility, the magnitude of the moment, and T_N near the phase boundary.²¹ The Fermi surface of κ -(BEDT-TTF)₂X has a two-dimensional nature, and the dimensionality does not change by applying pressure.²² Therefore the significant pressure dependence of β' -(BEDT-TTF)₂ICl₂ is connected to the dimensional crossover model. Additionally, the close vicinity of the superconducting and antiferromagnetic phases suggests that the superconductivity is intermediated by antiferromagnetic fluctuations, as predicted by the dimensional crossover model.^{1,7,19}

The quasi-one-dimensional character of β' -(BEDT-TTF)₂ICl₂ at ambient pressure is reminiscent of the similar behavior of the quasi-one-dimensional organic conductor (TMTTF)₂Br, in which T_N initially increases as pressure increases, then decreases with further pressure increases, and finally the superconductive transition occurs at

$T_c=0.8$ K under 2.6 GPa.^{23–25} This behavior is well explained not by the dimensional crossover model but by the quasi-one-dimensional correlated electron model. Therefore, β' -(BEDT-TTF)₂ICl₂ has the potential to be a high T_c quasi-one-dimensional superconductor.

The noticeable pressure dependence of the electron correlation should contribute to the magnetism. However, there is not significant change on the spin susceptibility and $(1/T_1T)^{-1}$ in the paramagnetic state from 0.6 to 2.1 GPa. The T_N of the salt more than doubles from 0.6 to 2.1 GPa, which is predicted by the dimensional crossover model, whereas J , which is estimated from the two-dimensional Heisenberg model, increases by only about 30%. Moreover, the one-dimensional Fermi surface in the salt is realized by the cancellation of interchain transfer integrals with different phases, whereas (TMTTF)₂Br has relative small interchain transfer integrals. The dimensional crossover model is based on the idea that this cancellation is sensitive to pressure. On the other hand, the simple band picture with an arbitrary number of dimensionalities cannot explain the nonmetallic behavior above T_N under pressure. Although the magnetic structure changed, the commensurate magnetic structure and large staggered moment under pressure cannot be fully explained by the nesting of Fermi surfaces. Further theoretical and experimental studies of band structure under pressure are desired. We expect that these problems can be resolved by

theoretical development, as well as by the development of a high-pressure NMR technique, up to 9 GPa.

In summary, using angular rotation NMR measurements, we could determine the hyperfine coupling tensor of β' -(BEDT-TTF)₂ICl₂. Using this result, we found that the amplitude of the antiferromagnetic moment was μ_B per dimer, strongly indicating that this salt is a dimer Mott insulator at ambient pressure, with one carrier per dimer. From NMR measurements made under pressure, we confirmed that the structure of the antiferromagnetic phase and the spin susceptibility changed significantly between ambient pressure and 0.6 GPa. In addition, T_N increased when a pressure of 0.6 GPa or higher was applied. This anomalous behavior was expected based on the dimensionality of the band picture. However, the simple band picture cannot explain the electrical conductivity and the commensurate antiferromagnetic structure under pressure. Theoretical development of both models of the salt is desired.

The authors wish to thank K. Kumagai and Y. Furukawa of Hokkaido University and H. Taniguchi of Saitama University for stimulating discussions. The authors also thank N. Matsunaga and K. Nomura of Hokkaido University for their help with high-pressure measurements. This work was supported in part by a Grant-in-Aid for Scientific Research (Grant No. 18540306) from the Ministry of Education, Culture, Sports, Science, and Technology.

*atkawa@phys.sci.hokudai.ac.jp

- ¹H. Kino and H. Kontani, *J. Phys. Soc. Jpn.* **67**, 3691 (1998).
- ²H. Kondo and T. Moriya, *J. Phys. Soc. Jpn.* **67**, 3695 (1998).
- ³J. Schmalian, *Phys. Rev. Lett.* **81**, 4232 (1998).
- ⁴H. Taniguchi, M. Miyashita, K. Uchiyama, K. Satoh, N. Mori, H. Okamoto, K. Miyagawa, K. Kanoda, M. Hedo, and Y. Uwatoko, *J. Phys. Soc. Jpn.* **72**, 468 (2003).
- ⁵N. Yoneyama, A. Miyazaki, T. Enoki, and G. Saito, *Synth. Met.* **86**, 2029 (1997).
- ⁶A. Matsunaga, S. Komiyama, Y. Noda, Y. Uwatoko, A. Kawamoto, and H. Taniguchi, *Abstract of JPS Meetings* **59**, 752 (2004).
- ⁷H. Kontani, *Phys. Rev. B* **67**, 180503(R) (2003).
- ⁸E. B. Yagubskii, I. F. Shchegolev, V. N. Laukhin, P. A. Kononovich, M. V. Karatsovnik, A. V. Zvarykina, and L. I. Buravov, *JETP Lett.* **39**, 12 (1984).
- ⁹V. A. Merzhanov, E. E. Kostyuchenko, V. N. Laukhin, R. M. Lobkovskaya, M. K. Makova, R. P. Shibaeva, I. F. Shchegolev, and E. B. Yagubskii, *JETP Lett.* **41**, 179 (1985).
- ¹⁰K. Murata, M. Tokumoto, H. Anzai, H. Bando, G. Saito, K. Kajimura, and T. Ishiguro, *J. Phys. Soc. Jpn.* **54**, 1236 (1985).
- ¹¹V. N. Laukhin, E. E. Kostyuchenko, Yu. V. Sushko, I. F. Shchegolev, and E. B. Yagubskii, *JETP Lett.* **41**, 81 (1985).
- ¹²M. Tokumoto, K. Murata, H. Bando, H. Anzai, G. Saito, K. Kajimura, and T. Ishiguro, *Solid State Commun.* **54**, 1031 (1985).
- ¹³S. Kagoshima, Y. Nogami, M. Hasumi, H. Anzai, M. Tokumoto, G. Saito, and N. Mori, *Solid State Commun.* **69**, 1177 (1989).
- ¹⁴J. M. Williams, H. H. Wang, M. A. Beno, T. J. Emge, L. M. Sowa, P. T. Copps, F. Behroozi, L. N. Hall, K. D. Carlson, and G. W. Crabtree, *Inorg. Chem.* **23**, 3839 (1984).
- ¹⁵H. H. Wang, M. A. Beno, U. Geiser, M. A. Firestone, K. S. Webb, L. Nunez, G. W. Crabtree, K. D. Carlson, J. M. Williams, L. J. Azevedo, J. F. Kwak, and J. E. Schirber, *Inorg. Chem.* **24**, 2465 (1985).
- ¹⁶H. Kobayashi, R. Kato, and A. Kobayashi, *Synth. Met.* **19**, 623 (1987).
- ¹⁷T. Mori and H. Inokuchi, *Solid State Commun.* **62**, 525 (1987).
- ¹⁸T. Mori, *Bull. Chem. Soc. Jpn.* **71**, 2509 (1998).
- ¹⁹T. Miyazaki, and H. Kino, *Phys. Rev. B* **68**, 220511(R) (2003).
- ²⁰M. Yamashita, A. Kawamoto, and K. Kumagai, *Synth. Met.* **133-134**, 125 (2003).
- ²¹K. Miyagawa, K. Kanoda, and A. Kawamoto, *Chem. Rev.* **104**, 5635 (2004).
- ²²J. Caulfield, W. Lubczynski, F. L. Pratt, J. Singleton, D. Y. K. Ko, W. Hayes, M. Kurmoo, and P. Day, *J. Phys.: Condens. Matter* **6**, 2911 (1994).
- ²³L. Balicas, K. Behnia, W. Kang, E. Canadell, P. Auban-Senzier, D. Jerome, M. Ribault and J. M. Fabre, *J. Phys. I* **4**, 1539 (1994).
- ²⁴B. J. Klemme, S. E. Brown, P. Wzietek, G. Kriza, P. Batail, D. Jerome, and J. M. Fabre, *Phys. Rev. Lett.* **75**, 2408 (1995).
- ²⁵S. E. Brown, B. J. Klemme, P. Wzietek, D. Jerome, and J. M. Fabre, *Synth. Met.* **86**, 1937 (1997).